ISSN 1330-3651 (Print), ISSN 1848-6339 (Online)
Received: 10 August 2025; Accepted: 22 November 2025

https://doi.org/10.17559/TV-20250810002897
Original scientific paper

Methodology for 3D Optimization of the Number and Locations of TLS Stations and Scanner Targets

Kornelija KLJEČANIN*, Marko PEJIĆ

Abstract: The study presents a methodology for 3D optimization of the number and arrangement of TLS stations and scanner targets. A hybrid approach is proposed, integrating the principles of classical geodetic 3D network design with the constraints of terrestrial laser scanning (incidence angle, complete object coverage, minimal overlap between adjacent point clouds), taking into account external obstacles, technical limitations, and the measurement characteristics of the scanner itself (accuracy of distance measurement, accuracy of horizontal and vertical deflection of the laser beam, minimum and maximum range). Previous studies have mostly focused on two-dimensional optimization of TLS station positions, neglecting height and real spatial obstacles. The effectiveness of the proposed approach was validated through application to a complex urban structure - the building of the Faculty of Architecture, Civil Engineering and Geodesy and the Faculty of Forestry at the University of Banja Luka. The results show that the presented optimization/planning methodology can significantly reduce the number of required positions for complete object scanning and the total number of scanner targets needed for reliable registration of all adjacent point clouds, while simultaneously improving the quality of the final 3D model and reducing field work time. This work also aims to contribute to the advancement of terrestrial laser scanning methodology and to lay the foundation for the development of automated tools for TLS data acquisition in urban environments.

Keywords: 3D optimization; accuracy; best scanner position; best target position; incidence angle; point cloud; registration; terrestrial laser scanning

1 INTRODUCTION

Terrestrial Laser Scanning (TLS) is a modern geodetic method for rapid and precise acquisition of spatial data on objects and terrain, through the generation of point cloud that represents a digital record of the scanned surface. By combining a laser range finder (distance meter), beam deflection system, and integrated sensors, modern scanners enable the generation of various 2D and 3D products such as digital terrain models, facade models. The quality and applicability of these products directly depend on the specifications of the TLS system, which include range, accuracy, resolution, field of view, and scanning speed.

Owing to its precision and flexibility, the quality of TLS-acquired data has demonstrated significant potential for application across diverse fields such as architecture, civil engineering, and structural design [1-3], mining and geology [4, 5], industrial inspection [6], archaeology [7, 8], forensics [9] as well as dentistry and medicine [10-14] among others. A particularly important area of TLS application is in the technical and deformation monitoring of infrastructure, where repeated scanning over different temporal epochs enables the determination of excavation and fill volumes [15, 16], terrain and structural settlements [17-20], deviations of as-built geometry from design specifications [21-23] and similar tasks.

However, to fully exploit the potential of TLS systems, careful planning of the scanning process is essential. For this reason, optimizing the number and spatial configuration of TLS stations represents a critical component of geodetic survey planning, aimed at achieving high accuracy and operational efficiency. To meet these objectives, several parameters must be balanced: minimizing the number of stations, ensuring complete object coverage, maintaining acceptable limits for laser beam incidence angles, and guaranteeing sufficient overlap between point clouds to ensure robust data registration.

The quality of terrestrial laser scanning is determined by four fundamental parameters [24]: 1) Measurement characteristics of the terrestrial laser scanner (range, accuracy of distance measurement, accuracy of horizontal and vertical deflection of the laser beam), 2) Surface properties of the scanned object (degree of surface reflectivity), 3) Environmental conditions during scanning (atmospheric pressure, humidity and air temperature, vibrations) and 4) Scanning geometry (incidence angle of the laser beam on the object surface and distance to the object).

The scanning geometry represents the parameter that can be most effectively influenced during the planning phase of terrestrial laser scanning. Data quality tends to decrease with increasing distance and laser beam incidence angle [25]. A key challenge lies in defining the optimal number and placement of scanning stations, as an inadequate configuration may result in insufficient point density, the presence of shadows, poor coverage, and reduced registration accuracy. Conversely, an excessive number of stations leads to increased costs, prolonged scanning time, and greater data processing efforts. Therefore, optimizing the scanning geometry is essential - it involves achieving a balance between the number of stations, object coverage, allowable incidence angles, and point cloud overlap to ensure high-quality registration.

The aim of this study is to explore possibilities for optimizing the number and arrangement of TLS stations, as well as the placement of scanner targets, with the objective of improving data quality, reducing fieldwork duration, and enhancing processing efficiency. The research builds upon existing mathematical and algorithmic models used in geodetic survey planning, with a particular focus on geometric and practical aspects of scanning under real-world conditions.

Related Work

Numerous previous studies have addressed the problem of determining the optimal number and arrangement of scanner stations for the complete scanning of an object or part of an object. Most approaches are based on the development of algorithms within the field of

computational geometry, which to varying degrees incorporate the specific characteristics and limitations of terrestrial laser scanning ([26-28]). Although TLS technology inherently involves the acquisition of spatial (3D) data, the planning process is most often carried out in a horizontal plane, i.e., within a two-dimensional (2D) coordinate system. Some approaches do not consider the overlap between neighbouring point clouds, fail to account for the technical specifications of the instrument, or neglect the stochastic nature of the scanning model. Moreover, when planning exterior scans of buildings, they often disregard obstacles outside the object, which are critical for generating feasible solutions.

A notable contribution to the optimization of TLS station number and location was presented by Y. Dehbi et al. [29]. The focus of the study is on indoor scan planning, which is conducted in a full 3D coordinate system. The work is based on the development of an algorithm to identify the minimum number of TLS stations required for complete scanning of interior surfaces (walls and floors), while accounting for obstacles and TLS limitations such as minimum and maximum scanner range and maximum allowable laser beam incidence angle. However, the optimization of the number and placement of scanner targets was not considered. The overlap between neighbouring TLS stations was addressed through the application of graph theory to ensure network connectivity.

The optimization of both the number and configuration of TLS stations and scanner targets for point cloud registration was explored by Fengman Jia in her doctoral dissertation defended in August 2019 [30]. The study focused on four buildings within the University of Calgary campus. The author introduced a hierarchical approach for selecting optimal scanner positions and employed a weighted greedy algorithm with variable resolution, which significantly improved computational efficiency, particularly in cases involving complex building geometries. The space surrounding the objects was treated as an open area without obstacles, and interactions with adjacent structures were not taken into account. The overlap between neighbouring TLS stations was not considered, and all computations were carried out in a two-dimensional coordinate system.

The study by the same author, proposes a practical strategy for the optimal placement of TLS devices [27]. The goal of the method is to reduce the number of required scanning stations while ensuring complete scene coverage. The approach was developed to enable efficient exploration of the solution space, taking into account the complexity of the environment. The proposed algorithm was tested on 540 simulated polygons of varying sizes and complexity levels. Compared to a benchmark strategy, the analysis demonstrated that the new algorithm yielded equally good or better results in 85.6% of cases. For more complex scenarios, the method showed potential to reduce project costs by up to 10%. Although the algorithm may show slightly lower efficiency in some instances, it still provides solutions within a few minutes for polygons with up to 500 vertices, making it suitable for practical applications under real-world conditions.

2 MATERIALS AND METHODS

The optimization of the TLS station network and scanner targets is based on multi-criteria system optimization, subject to constraints in both the feasible set and the criteria function space, incorporating decision-maker preferences.

The mathematical model for optimizing the number and distribution of TLS stations and scanner targets is built upon the mathematical relationship between polar and Cartesian coordinates, even in the absence of original observed values for distances, horizontal directions and vertical angles [25]:

$$\begin{aligned} \rho_{ij} &= \sqrt{\Delta x_{ij}^2 + \Delta y_{ij}^2 + \Delta z_{ij}^2}, \\ \alpha_{ij} &= \arcsin\left(\frac{\Delta z_{ij}}{\sqrt{\Delta x_{ij}^2 + \Delta y_{ij}^2 + \Delta z_{ij}^2}}\right), \\ \theta_{ij} &= \operatorname{arctg}\left(\frac{\Delta y_{ij}}{\Delta x_{ij}}\right). \end{aligned} \tag{1}$$

The mathematical model used for the optimization is the indirect adjustment model [31]:

$$\left.\begin{aligned} &\text{Linear}: \quad v = Ax + f, \quad M\left[f\right] = -Ax, \\ &\qquad\qquad \text{with constraint } R^T x = 0, \\ &\text{Stochastic}: \quad M\left[v\right] = 0, \quad M\left[vv^T\right] = K = \sigma^2 \cdot P^{-1}, \end{aligned}\right\} \tag{2}$$

where: x - is the vector of network point coordinates, A - is the design matrix (defining the geometry of the network), R - is the a priori variance-covariance matrix of the planned observations (distances, horizontal directions, and vertical angles)), f - is the vector of constants (free terms) in the observation equations, v - is the vector of residuals, σ^2 - is dispersion (variance), P - is the weight matrix of the planned observations.

For the optimization of the number and spatial distribution of TLS stations and scanner targets, a feasible set W is defined, subject to the following constraints:

$$\begin{aligned} &1° \quad P_i > 0, \\ &2° \quad R_{ii} - 0.20 \geq 0, \ i = 1, 2, ..., \left(n_\rho + n_\theta + n_\alpha\right) \\ &3° \quad 7.65 - \frac{G_i^*}{\sigma_i} \geq 0, \end{aligned} \tag{3}$$

where: n_ρ - is the number of planned distance observations, n_θ - is the number of planned horizontal direction observations, n_α - is the number of planned vertical angle observations, σ_i - are the variances of the planned observations (distances, horizontal directions, and vertical angles), P - are the corresponding weight values assigned to the planned observations, R_{ii} - are the internal reliability coefficients of the planned observations, G_i^* - is the marginal gross error that can be reliably detected in the observation using the Data Snooping test. The expression used to compute the marginal gross error is given by the following formula [32]:

$$G_i^* = \frac{\sigma_i \sqrt{\lambda_0}}{\sqrt{R_{ii}}} = \frac{\sigma_i \cdot \left(t_{1-\beta_0} + t_{1-\alpha_0/2}\right)}{\sqrt{R_{ii}}}, \tag{4}$$

where: $t_{1-\beta_0}$, $t_{1-\alpha_0/2}$ - are quantiles of the standard normal distribution corresponding to significance level α_0 and detection probability $1-\beta_0$, λ_0 - is the non-centrality parameter of the non-central normal distribution used in local gross error detection tests. In the design of geodetic networks, a detection power of 0.8 is generally considered high, and thus a value of is adopted, [31]. Regarding the significance level no consensus exists on a universally accepted value. A level of 0.05 is stricter than 0.001, and it is recommended to use $\alpha_0 = 0.001$ in calculations for robust outlier detection.

According to Perović [31], a vector-valued objective function is formulated with the following components, adapted to the specific requirements of terrestrial laser scanning:

$$\begin{aligned} &f_1(w) = \overline{R} = \frac{n - r(A)}{n}, \; f_3(w) = \arccos\left(\frac{P_i \cdot N}{|P_i| \cdot |N|}\right), \\ &f_2(w) = \frac{A_j}{B_j}, \qquad\qquad f_4(w) = \frac{N_{\text{obs}}}{N_{\text{all}}}, \end{aligned} \tag{5}$$

for which the minimum and maximum are sought, $\min f_k(w), \forall k \in (1, 2, 3)$ and $\max f_4(w)$, subject to the following constraints in the criterion function domain:

$$\begin{aligned} &1^\circ \quad \overline{R} - R_{\text{opt}} \geq 0 \qquad\qquad 3^\circ \quad \alpha_{\max} - \alpha_i \geq 0, \\ &2^\circ \quad 2 - \frac{A_j}{B_j} \geq 0, 2 - \frac{A_j}{C_j} \geq 0 \qquad 4^\circ \quad N_{\text{all}} - N_{\text{obs}} = 0, \end{aligned} \tag{6}$$

where: $\overline{R}$ - is mean coefficient of internal reliability, R_{opt} - is optimal value of the internal reliability coefficient, A_j, B_j, C_j - is semi-axes of the triaxial error ellipsoid, α_i - is incidence angle of the laser beam, $\alpha_{\max}$ - is maximum allowable incidence angle, - is vector from the TLS to the point on the object surface hit by the emitted laser beam, N - is vector normal to the tangent of the object surface at the point where the incidence angle is calculated, N_{all} - is total number of segments into which the object is discretized, N_{obs} - is number of visible segments.

The process of TLS network optimization can be briefly described in three steps, according to the methodology for geodetic network optimization adapted to the specific characteristics and requirements of terrestrial laser scanning technology. To clearly illustrate the TLS scan planning optimization procedure, Fig. 1 presents a flowchart (diagram) encompassing all relevant phases, including iterative adjustments aimed at achieving maximum measurement efficiency and data quality.

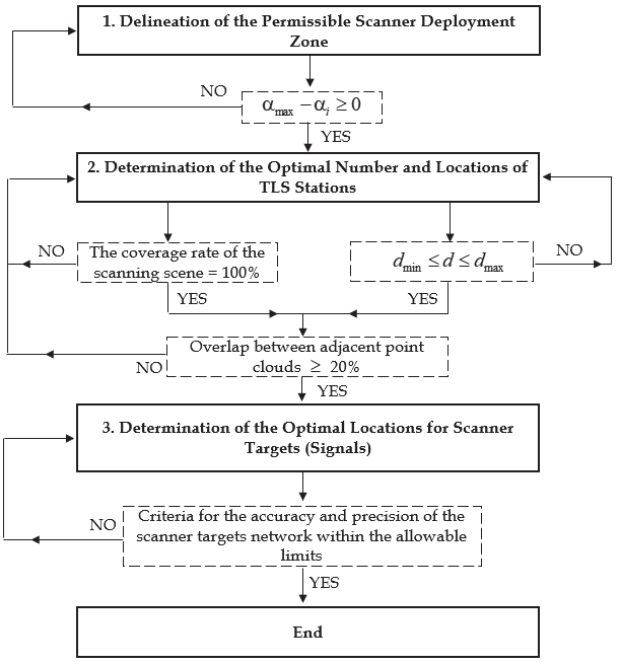

Figure 1 Flowchart of the proposed method for optimizing the number and locations of terrestrial laser scanner stations and scanner targets

2.1 Delineation of the Permissible Scanner Deployment Zone - Step K1

In the process of selecting optimal TLS station locations, the presence of environmental obstructions, such as adjacent structures, vegetation, and other physical barriers, often constrains the achievable network geometry. These limitations can significantly impair the spatial distribution of observations and result in suboptimal incidence angles of the laser beam upon the target surface. To mitigate such effects, the permissible scanner deployment zone is rigorously defined by incorporating both external obstructions and the geometric constraint expressed in Eq. (6-3). Specifically, this involves the delineation of two critical boundaries: (1) the maximum permissible distance from the scanner to the object ensuring unobstructed scanning visibility, and (2) the minimum permissible proximity of the scanner to the object, governed by the allowable upper bound of the laser beam's incidence angle. This approach ensures that the scanning configuration remains within the operational envelope necessary for high-precision data acquisition and minimizes systematic errors induced by unfavourable scanning geometries.

2.2 Selection of the Optimal Number and Locations of TLS Stations - Step K2

Within the previously defined permissible scanner deployment zone, the decision-maker is tasked with determining both the optimal number and spatial arrangement of terrestrial laser scanner stations. The goal is to minimize the total number of stations while ensuring sufficient overlap between adjacent point clouds and achieving complete coverage of the object or the designated section thereof (Eq. (6-4)). The station positions must be iteratively adjusted until Eq. (6-4) is satisfied, with the additional requirement that all stations remain within

the defined permissible area. Furthermore, both the minimum and maximum effective ranges of the scanner must be considered during planning. To assess the extent of object coverage, the object is discretized into planar segments of predefined length. For each TLS station, a visibility matrix is generated, which serves as the basis for evaluating the degree of coverage. The coverage metric is calculated using the following expression [30, 33]:

$$E[\%] = \left(\frac{N_{\text{obs}}}{N_{\text{all}}} \right) \cdot 100, \tag{7}$$

where: N_{all} - is the total number of discretized segments, N_{obs} - is the number of visible segments.

An approximate value of the overlap between adjacent point clouds can be computed by analyzing the relative positions of scanner stations in the horizontal plane. For instance, in order to ensure at least 20% overlap between neighbouring point clouds, a TLS unit with a maximum range of 80 m must provide a shared scanned surface area exceeding 4000 m² [29].

An increase in both the incidence angle and the scanner-to-object distance leads to a reduction in the return signal intensity, thereby degrading scan quality [34-36]. The precision of range measurements significantly deteriorates when the incidence angle exceeds a critical threshold [36-39].

According to Pejić [25], the optimization criterion for the laser beam incidence angle is based on the principle of negligibility of the angular contribution to the variance of TLS distance measurements. By applying this principle, specifically, by neglecting the component of measurement uncertainty attributable to the incidence angle, assuming a negligibility coefficient is concluded that the maximum allowable incidence angle amounts to 78°.

2.3 Selection of the Optimal Number and Locations of Scanner Targets (Signals) - Step K3

The decision-maker determines the number, spatial arrangement, and type of scanner targets. These targets may be positioned directly on the surface of the object or in its immediate surroundings, placed at varying heights and distances relative to the TLS station. Targets used within the overlap zones of adjacent point clouds must not be collinear, as such configurations adversely affect the geometric robustness of the registration process. The optimal number of scanner targets for reliable registration is three (3), when combined with the cloud-to-cloud registration method (i.e., surface-based best-fit alignment). If the instrument is equipped with a dual-axis tilt compensator, the optimal number of targets is reduced to two (2), assuming that cloud-to-cloud registration is also employed.

The choice of the number and type of traditional geodetic observations is irrelevant in this context, as direct targeting during TLS data acquisition is not feasible. The primary observables in a TLS network are range (distance), horizontal direction, and vertical angle. Each scanner target must be observed from at least two TLS stations. Consequently, for n scanner targets, a system of at least 6n observation equations is established, comprising 2n distances, 2n horizontal directions, and 2n vertical angles, with 3*n* unknown parameters (i.e., coordinate corrections of the scanner targets). Additionally, coordinate corrections of the TLS stations are introduced into the system of adjustment equations as unknowns.

The weights of the measured quantities are computed based on the principle that the standard deviations of horizontal directions and vertical angles (expressed through their linear equivalents) are assumed to be equal to the standard deviations of distance measurements [31]:

$$P_\rho = \frac{\sigma_0^2}{\sigma_\rho^2} \text{ - weight for distance measurements,} \tag{8}$$

$$P_\theta = \frac{\sigma_0^2}{\left(\frac{\sigma_\rho}{\rho_H} \cdot \rho'' \right)^2} \tag{9}$$

- weight for horizontal direction measurements,

$$P_\alpha = \frac{\sigma_0^2}{\left(\frac{\sigma_\rho}{\rho} \cdot \rho'' \right)^2} \tag{10}$$

- weight for vertical angle measurements.

The weight matrix, *P*, is a square matrix whose dimensions depend on the total number of planned mutually independent observations. The diagonal elements of the weight matrix are computed according to Eqs. (8), (9) and (10), while all off-diagonal elements are equal to zero:

$$P_{\left[\left(n_\rho + n_\theta + n_\alpha \right) x \left(n_\rho + n_\theta + n_\alpha \right) \right]} = \begin{bmatrix} P_p & 0 & 0 \\ 0 & P_\theta & 0 \\ 0 & 0 & P_\alpha \end{bmatrix}. \tag{11}$$

After the weight matrix is constructed, the observation reliability matrix *R* is computed [40]:

$$R = E - A\left(A^T P A \right)^+ A^T P, \tag{12}$$

where: *A* - is design matrix, *E* - identity matrix. The diagonal elements of the matrix *R* represent the internal reliability coefficients of the planned observations $\left(R_{ii} \right)$. The mathematical expressions for computing the elements of the matrix *A* are given as follows:

$$\begin{aligned} a_{ij} &= \left(\frac{\partial \theta_{ij}}{\partial x_i} \right)^0 = \frac{\sin \theta_{ij}^0}{\rho_{H_{ij}}^0} \cdot \rho'', \\ b_{ij} &= \left(\frac{\partial \theta_{ij}}{\partial y_i} \right)^0 = -\frac{\cos \theta_{ij}^0}{\rho_{H_{ij}}^0} \cdot \rho'', \\ c_{ij} &= \left(\frac{\partial \theta_{ij}}{\partial z_i} \right)^0 = 0, \end{aligned} \tag{13}$$

- coefficients for horizontal directions,

$$A_{ij}=\left(\frac{\partial\rho_{ij}}{\partial x_i}\right)^0=-\cos\theta_{ij}^0\cdot\cos\alpha_{ij}^0,$$
$$B_{ij}=\left(\frac{\partial\rho_{ij}}{\partial y_i}\right)^0=-\sin\theta_{ij}^0\cdot\cos\alpha_{ij}^0, \quad (14)$$
$$C_{ij}=\left(\frac{\partial\rho_{ij}}{\partial z_i}\right)^0=-\sin\alpha_{ij}^0,$$

-coefficients for distances,

$$e_{ij}=\left(\frac{\partial\alpha_{ij}}{\partial x_i}\right)^0=\frac{\cos\theta_{ij}^0\cdot\sin\alpha_{ij}^0}{\rho_{ij}^0}\cdot\rho'',$$
$$f_{ij}=\left(\frac{\partial\alpha_{ij}}{\partial y_i}\right)^0=\frac{\sin\theta_{ij}^0\cdot\sin\alpha_{ij}^0}{\rho_{ij}^0}\cdot\rho'', \quad (15)$$
$$g_{ij}=\left(\frac{\partial\alpha_{ij}}{\partial z_i}\right)^0=-\frac{\cos\alpha_{ij}^0}{\rho_{ij}^0}\cdot\rho''.$$

- coefficients for vertical angles.

The dimensions of the design matrix A depend on the number of planned observations and the number of unknown points in the TLS network.

The values of the semi-axes of the triaxial error ellipsoid are given in [40]:

$$A=\sigma_0\sqrt{2\sqrt{\left(-\frac{p}{3}\right)}\cdot\cos\left(\frac{\varphi}{3}\right)-\frac{a}{3}}, \quad (16)$$

$$B=\sigma_0\sqrt{2\sqrt{\left(-\frac{p}{3}\right)}\cdot\cos\left(\frac{\varphi+2\pi}{3}\right)-\frac{a}{3}}, \quad (17)$$

$$C=\sigma_0\sqrt{2\sqrt{\left(-\frac{p}{3}\right)}\cdot\cos\left(\frac{\varphi+4\pi}{3}\right)-\frac{a}{3}}, \quad (18)$$

where: $p=b-\frac{a^2}{3}$, $q=c-\frac{a\cdot b}{3}+\frac{2a^3}{27}$,

$\varphi=\arccos\left(\frac{-q}{2\sqrt{(-p/3)^3}}\right)$, $a=-\left(Q_{xx}+Q_{yy}+Q_{zz}\right)$,

$b=Q_{xx}\cdot Q_{zz}+Q_{yy}\cdot Q_{zz}+Q_{xx}\cdot Q_{yy}-Q_{xy}^2-Q_{xz}^2-Q_{yz}^2$,

$Q_x=\left(A^TPA\right)^+$ - the cofactor matrix of the unknown parameters (where the unknown parameters are the coordinate increments of the points), $c = Q_{xx}\cdot Q_{yz}^2+Q_{yy}\cdot Q_{xz}^2+Q_{zz}\cdot Q_{xy}^2-Q_{xx}\cdot Q_{yy}\cdot Q_{zz}-2Q_{xy}\cdot Q_{xz}\cdot Q_{yz}$.

The selected positions of TLS stations and scanner targets must satisfy Eqs. (3-1), (3-2), (3-3), (6-1) and (6-2). If any of the aforementioned constraints are not fulfilled, the decision-maker must adjust the positions of both the TLS stations scanner targets until the constraints are met. It is essential to verify whether any of the constraints from the previous steps have been violated during the relocation process - specifically, whether the stations remain within the permissible scanner deployment zone and whether the requirement for complete coverage of the object (or its designated section) is still satisfied.

By following steps K1, K2, and K3, Eqs. (3-1), (3-2), and (3-3) are satisfied within the admissible set, while Eqs. (6-1), (6-2), (6-3), and (6-4) are fulfilled within the criterion function space, thus concluding the optimization process.

3 THE PRACTICAL CASE STUDY

The practical case study presented in this work involved the definition of optimization criteria for scanning a complex architectural structure located within the urban area of the Faculty of Architecture, Civil Engineering and Geodesy, and the Faculty of Forestry at the University of Banja Luka. During the scanning process, an optimized plan was implemented, which included the reduction of the number of scanner stations, optimal spatial arrangement of the stations, selection of appropriate parameters (such as resolution and scan angle), and the use of software tools to minimize scan overlap and acquisition time. This case study demonstrates the practical application of theoretical principles for TLS scan planning optimization, emphasizing their relevance for improving the efficiency and accuracy of measurements in architectural and urban surveying practice.

3.1 Determination of the Admissible Area for Scanner Placement

The target object for which scan planning is required is the building of the Faculty of Architecture, Civil Engineering and Geodesy and the Faculty of Forestry at the University of Banja Luka (Fig. 2). The building is located within the former Vrbas military complex, now part of the University Campus in Banja Luka. The area managed by the University of Banja Luka is characterized by landscaped park structures, grass-covered surfaces, and protected dendrological assets.

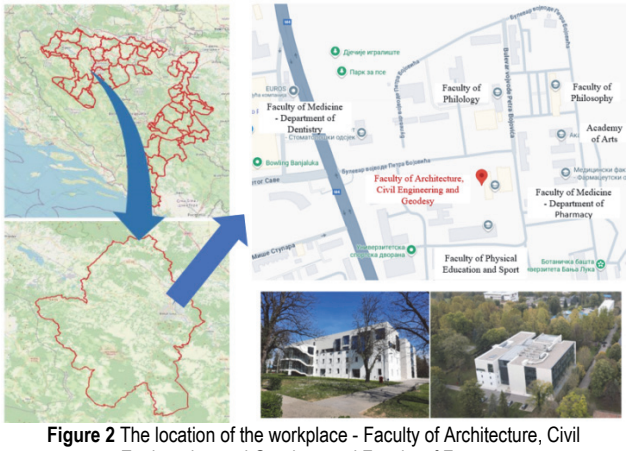

Figure 2 The location of the workplace - Faculty of Architecture, Civil Engineering and Geodesy and Faculty of Forestry

In the vicinity of the Faculty of Architecture, Civil Engineering and Geodesy and the Faculty of Forestry building, a significant number of trees are present, which complicates the scanning process. To facilitate the planning of terrestrial laser scanning operations, field data

on physical obstacles were collected. As shown in Fig. 5, the unobstructed scanning area is delineated by a blue boundary line, which defines the maximum extent within which the terrestrial laser scanner can be positioned to allow for unobstructed scanning.

The incidence angle of the laser beam is defined as the angle formed between the laser beam and the surface normal of the object being scanned. The value of the laser beam incidence angle can be calculated using the following expression [41]:

$$\alpha_i = \arccos\left(\frac{P_i \cdot N}{|P_i| \cdot |N|}\right), \tag{19}$$

where: $P_i = (x_i, y_i, z_i), i = 1, 2, ..., m$ - is the vector from the TLS device to the point i on the object surface struck by the emitted laser beam; N - is the vector normal to the tangent of the surface at that point i. The incidence angle may range from 0° to 360°.

When the laser beam strikes the object surface at a right angle (normal incidence), the laser footprint assumes a circular shape. In contrast, at arbitrary (oblique) incidence angles, the laser footprint becomes elliptical, which leads to a decrease in the intensity of the return signal and a reduction in the signal-to-noise ratio (SNR), ultimately increasing the uncertainty of the distance measurement.

For each side of the object, the minimum permissible distance of the terrestrial laser scanner was determined based on the maximum allowable incidence angle, following the approach illustrated in Fig. 4. Depending on the architectural design, building facades may be flat or feature protruding elements such as staircases, terraces, balconies, or bay windows. The buildings of the Faculty of Architecture, Civil Engineering and Geodesy and the Faculty of Forestry have a more complex structural configuration. The following section describes the procedure for determining the limiting proximity boundary, i.e., the closest distance to the object at which the scanner may be positioned on one side of the faculty building.

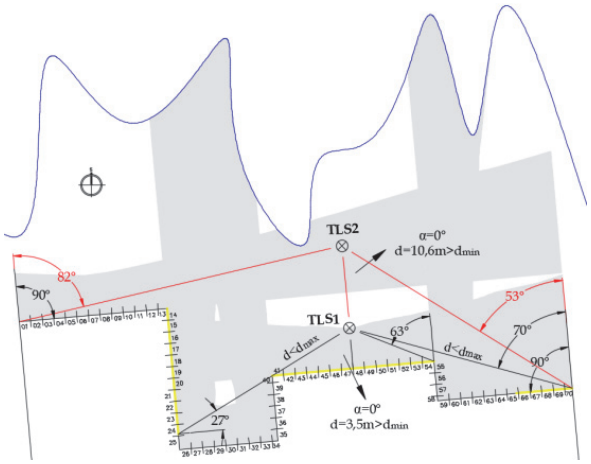

Figure 1 2D representation of the maximum permissible proximity of the scanner to the object at an incidence angle of 78°. The incidence angle values for boundary cases are indicated. The portion of the object visible from TLS station 1 is shown in yellow. The blue line represents the maximum allowable scanner distance, constrained by obstacles in the environment. The gray-shaded area denotes the zone within which scanner placement is not permitted

Fig. 3 presents a 2D representation of the maximum allowable scanner proximity to the object, corresponding to a predefined maximum incidence angle of the laser beam $(\alpha_{\max} = 78°)$. The objective is to select a scanner location such that, for every visible segment of the building, the incidence angle does not exceed the defined threshold of 78°, and the beam length remains within the scanner's operational range, neither exceeding the maximum range nor falling below the minimum. The incidence angle was calculated for the farthest visible point on the building's facade using Eq. (19), considering the total building heigh $(\approx 15\ \text{m})$. Based on this geometry, the maximum allowable incidence angle is calculated to be ≈ 78° in the vertical plane and 63° in the horizontal plane. For the selected scanner position (station TLS1), the minimum permissible distance to the object is 3.5 meters, at which point the laser beam strikes the surface at a normal angle $(\alpha = 0°)$. The area of the object visible from TLS1 is highlighted in yellow. From TLS1, a total of 30 segments out of 70 are visible, corresponding to a coverage rate of 43% for the observed side of the object.

Fig. 3 also shows a suboptimal scanner location (station TLS2). For several segments visible from TLS2, the incidence angle exceeds the defined maximum allowable value 78° . It is evident from the figure that station TLS2 lies outside the admissible TLS deployment area.

The observed side of the Faculty of Architecture, Civil Engineering and Geodesy and the Faculty of Forestry building is not flat; rather, it consists of a combination of protruding and recessed segments (Fig. 4). At one-meter intervals along the facade (and at even finer intervals in certain sections), a maximum permissible proximity line is drawn for each individual segment of the observed side. This line ensures that the maximum incidence angle does not exceed and that the constraints related to the scanner's minimum and maximum range are satisfied (Fig. 4). In this way, a restrictive zone is defined for each segment within which scanner placement is not allowed. By intersecting the restrictive zones defined for all individual segments, a composite limiting area is obtained. This area represents the space within which scanner positioning is not permitted for scanning the observed side of the building, in compliance with Eq. (6-3).

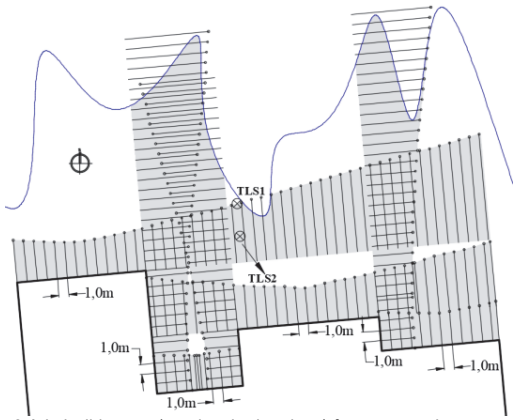

Figure 2 Admissible area (non-hatched regions) for scanner placement on one side of the object at an incidence angle of α_{max} = 78°. The blue line represents the maximum allowable scanner distance for unobstructed scanning of the object

The procedure described above was applied to all four sides of the faculty building, with upper boundary values for the incidence angle set at 65° and 78°. In Fig. 5 and Fig. 6, the non-hatched/unshaded areas outside the object represent the area of permissible instrument placement depending on the maximum allowable value of the incidence angle (Eq. (9-3)) and obstacles in the field, i.e., the admissible area for scanner placement. The line of the limiting space to which the scanner can be placed for unobstructed scanning of the object, and the line of the limiting space to which the scanner can approach the object the closest - depending on the maximum allowable incidence angle of the laser beam and the minimum and maximum range of the available terrestrial laser scanner - define the admissible instrument placement area. If a scanner station is positioned within this admissible area, it can be assured that for every visible part of the object, the incidence angle will not exceed the predefined maximum value, and the scanning process can proceed without obstruction.

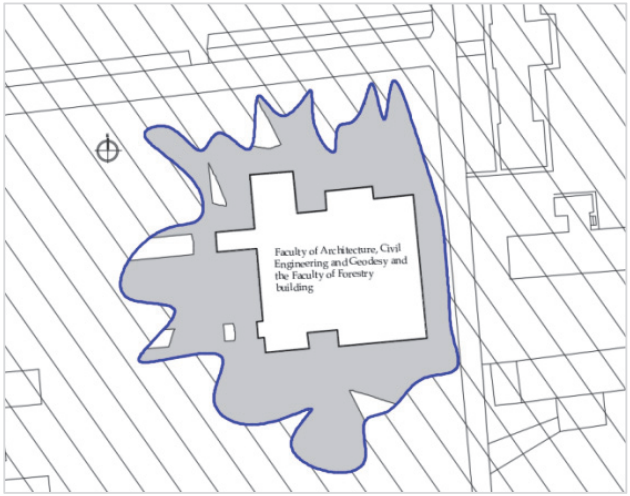

Figure 3 Admissible area (non-hatched regions outside the object) for scanner placement for scanning the building of the Faculty of Architecture, Civil Engineering and Geodesy and the Faculty of Forestry at an incidence angle of α_{max} = 65°. The blue line represents the maximum allowable scanner distance, determined based on obstacles present in the field

Figure 4 Admissible area (non-hatched/unshaded regions outside the object) for scanner placement at an incidence angle of α_{max} = 78°. for the building of the Faculty of Architecture, Civil Engineering and Geodesy and the Faculty of Forestry

However, at an upper incidence angle limit of 65°, it is not possible to configure the TLS station layout such that Eq. (6-4) is satisfied - i.e., full coverage of the Faculty of Architecture, Civil Engineering and Geodesy and the Faculty of Forestry building cannot be achieved under this condition (Fig. 5).

The maximum value of the laser beam incidence angle on the object surface is set to. TLS stations must be positioned within the unshaded/non-hatched areas outside the object (Fig. 6) in such a way that the number of stations is minimized, the entire object is fully scanned, sufficient overlap between point clouds is ensured, and the distance between the scanner and the object remains within the allowable limits.

3.2 Determination of the Optimal Number and Locations of TLS Stations

TLS stations are distributed within the admissible scanner placement area in such a way that the number of stations is minimized, sufficient overlap between adjacent point clouds is ensured, the scanner's minimum and maximum range constraints are not violated $(d_{\min} < d < d_{\max})$, and the entire object is fully scanned.

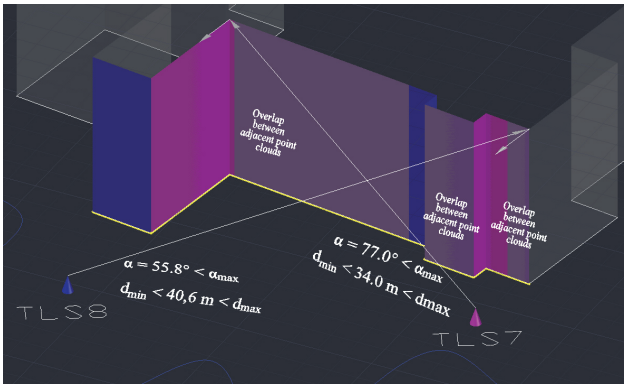

Figure 5 Maximum incidence angle (< 78°) and slant distance from TLS7 and TLS8 to the object. The part of the object visible from both TLS7 and TLS8 is shown in purple (> 20%), the part visible only from TLS8 is shown in blue, and the part visible only from TLS7 is shown in magenta. The coverage rate of the extracted part of the building, indicated by a yellow line, amounts to 100%.

The proposed optimal configuration and number of TLS stations is shown in Fig. 8. It is planned that two sides of the faculty building will be scanned from five TLS stations (stations labelled TLS5, TLS6, TLS7, TLS8, and TLS9).

The two building sides were discretized into 146 segments $(N_{all} = 146)$, each one meter in length. The number of segments visible from the five TLS stations is $146\,(N_{obs} = 146)$, and according to Eq. (7), the coverage rate of the object is 100%. Therefore, the station configuration shown in Fig. 8 ensures complete scanning of the object, thereby satisfying Eq. (6-4).

Considering that the scanning is planned to use a scanner with a maximum range of 70 meters, the shared scanning area between two adjacent TLS stations must be greater than 3,080 m² to achieve a minimum overlap of 20% between neighbouring point clouds. In the present case, the approximate overlap exceeds 40%, ensuring sufficient overlap between adjacent scans.

Tab. 1 presents the maximum incidence angle values and the slant distances from the instrument to the object for each TLS station shown in Fig. 8, considering the instrument height $(i \approx 1.5\ \text{m})$.

Table 1 Maximum incidence angle and slant distance from TLS to the object

TLS Station	Maximum Incidence Angle in 2D / °	Maximum Incidence Angle in 3D / °	Maximum Slant Distance / m
TLS5	71.7	72.6	43.5
TLS6	67.4	70.8	39.9
TLS7	75.8	77.0	34.0
TLS8	53.4	55.8	40.6
TLS9	58.2	69.0	19.4

3.3 Determination of Optimal Locations for Scanner Targets

To register adjacent point clouds acquired by scanning two sides of the Faculty of Architecture, Civil Engineering and Geodesy and the Faculty of Forestry building from five TLS stations, a total of eight scanner targets were defined within the vicinity of the structure, one target mounted on the object surface, and seven positioned outside the object (Fig. 8). The proposed configuration of scanner targets satisfies the non-collinearity condition, ensuring that at least three common targets are visible from each pair of neighbouring TLS stations.

The scanning is planned to be performed using a Faro FocusM terrestrial laser scanner. The Faro FocusM belongs to the category of phase-based scanners, with the distance measurement principle based on phase shift measurement. The scanner has a declared range of 0.6 m to 70 m, and a specified distance accuracy of ±3 mm $(\sigma_\rho = \pm 3\,\text{mm})$. Due to the scanner's construction, the area directly beneath the instrument is not scanned, meaning that in the horizontal plane, the scanner does not describe a full 360° field of view, but rather 300°. In the vertical plane, the scanner provides a full 360° field of view.

Table 2 Local coordinates of 3D TLS network points of the faculty building

Point	Y_0 / m	X_0 / m	H_0 (Z_0) / m
TLS5	8 017.2143	161.6044	1.50
TLS6	7 994.5202	160.4628	1.50
TLS7	7 975.7018	174.3455	1.50
TLS8	7 957.8428	203.4733	1.50
TLS9	7 968.5986	214.6623	1.50
OB3	7 981.3913	196.5089	0.50
5	8 005.8386	157.1967	0.00
6	8 005.3641	172.8658	0.00
7	7 987.0067	168.0728	0.00
8	7 966.274	180.4692	0.00
9	7 962.6134	190.5669	0.00
10	7 963.0107	209.7556	0.00
11	7 977.1440	215.6445	0.00

According to Eqs. (8), (9) and (10), the diagonal elements of the weight matrix P are determined. This is followed by the computation of the observation reliability matrix R, in accordance with (12), and the evaluation of the internal reliability coefficients for the planned observations. The lowest value of the internal reliability coefficient for the TLS network design shown in Fig. 8 is 0.30, which is greater than the permissible value $\left(\min\left(R_{ii}\right) = 0.30 \geq 0.20\right)$, thus satisfying constraint (3-2).

The mean internal reliability coefficient is 0.66. Since this value exceeds the required minimum $\left(\overline{R} = 0.66 > 0.40\right)$, constraint (6-1) is also satisfied.

The marginal detectable error is computed using Eq. (4). The maximum value of the ratio $\frac{G_i^*}{\sigma_i}$ (i.e., the ratio of the marginal error to the standard deviation of the planned observation) is 6.22, which is less than the allowable limit $\left(\max\left(\frac{G^*}{\sigma}\right) = 7.65\right)$, thereby satisfying constraint (3-3).

The semi-axes of the 3D error ellipsoid are calculated using Eqs. (16), (17) and (18). The maximum ratio of the semi-axes A to B is 1.82 $\left(\max\left(A_0/B_0\right) = 1.82 < 2\right)$ and the maximum ratio of A to C is 1.49 $\left(\max\left(A_0/C_0\right) = 1.49 < 2\right)$. These values do not exceed the permissible limits, thus satisfying constraint (6-2).

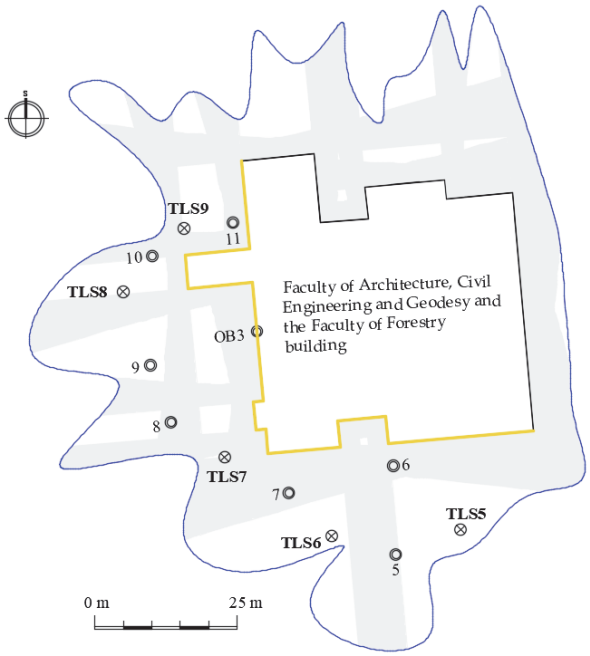

Figure 6 Optimal configuration and number of TLS stations and scanner targets for scanning two sides of the Faculty of Architecture, Civil Engineering and Geodesy and the Faculty of Forestry building. The two building sides subject to scan planning are indicated by yellow lines.
⊗ - TLS station, ◎ - spherical scanner target.

At the target location labelled OB3, which is planned to be stabilized directly on the object, a spherical target was used. This decision is based on the fact that from station TLS7, the incidence angle of the laser beam toward this target exceeds the maximum permissible value for the reliable recognition of a flat target.

For the configuration of TLS stations and scanner targets shown in Fig. 8, all defined Eqs. (3-1), (3-2), (3-3), (6-1) and (6-2) are fulfilled.

4 VALIDATION OF THE PROPOSED TLS GEOMETRY OPTIMIZATION METHODOLOGY - EXPERIMENTAL RESULTS

The scanning of the two facades of the Faculty of Architecture, Civil Engineering and Geodesy and the

Faculty of Forestry was conducted according to four distinct scanning plans. Each plan was designed with varying constraints related to target configuration, station layout, scanning resolution, and scanning duration. The objective was to evaluate the proposed TLS optimization methodology against conventional and reduced configurations.

1. Plan I - Experience-Based Scanning Configuration: This plan was designed based on the authors' prior field experience, while complying with key operational constraints: minimum point cloud overlap, scanner range limits, full coverage of the object, and a minimal number of TLS stations. The two facades were scanned using five TLS stations, with eight spherical and thirteen flat targets placed on the building and in the surrounding area. The total scanning duration was 155 minutes (5 stations × 31 minutes per station). A dual-axis tilt compensator was active throughout the process.
2. Plan II - Proposed Optimization-Based Configuration: This plan was derived using the proposed TLS geometry optimization methodology (Fig. 8). Three spherical targets were strategically placed within the overlap regions between adjacent point clouds, in accordance with quality constraints for 3D geodetic networks. The building was scanned from five TLS stations (TLS5, TLS6, TLS7, TLS8, TLS9), and eight spherical targets (IDs: 5, 6, 7, 8, 9, 10,11, OB3) were used for complete registration. The maximum distance to any target ranged between 19 m and 35 m. Using the scanner's Resolution - 1/2 mode, each station required 31 minutes, resulting in a total scanning time of 155 minutes. A dual-axis compensator remained active during scanning.
3. Plan III - Reduced Target Configuration: As shown in Fig. 9a, the number and locations of TLS stations remained identical to Plan II (TLS5, TLS6, TLS7, TLS8, TLS9). Only two targets were used per overlapping zone, totalling five spherical targets (IDs: 6, 7, 9, 10, OB3). The locations of the common scanner targets are identical to those in Plan II. The object was scanned from five TLS stations over 155 minutes. A dual-axis tilt compensator was active during the acquisition.
4. Plan IV - Mixed Resolution and Target Minimization Strategy: Also shown in Fig. 9b, the number and locations of TLS stations remained identical to Plan II (TLS5, TLS6, TLS7, TLS8, TLS9). Only two targets were used per overlapping zone, totalling seven spherical targets (IDs: 5, 6, 7, 9, 10, 11, OB3). The locations of the common scanner targets are identical to those in Plan II. For TLS5, TLS6, and TLS9, the maximum distance to the nearest target did not exceed 19 m, allowing each scan to be completed within 10 minutes using Resolution - 1/4. For TLS7 and TLS8, where the distance exceeded 19 m but remained below 35 m, scans required 31 minutes (Resolution - 1/2). The total scanning time for Plan 4 was 92 minutes (3 × 10 minutes + 2 × 31 minutes). A dual-axis tilt compensator was active during the acquisition.

Prior to scanning, all required scanner targets were installed to enable point cloud registration. Since the total number of targets varied across the scanning plans, field preparation time also differed. Consequently, preparation time was included as a comparative parameter in the evaluation of the scanning plans (Tab. 3).

According to the fourth scanning plan, the two facades were scanned in 92 minutes, i.e., 63 minutes less than under the remaining three plans; therefore, scanning time was treated as a key comparison parameter (Tab. 3).

Data processing was carried out in FARO SCENE 3D Point Cloud Software, using a combination of two registration methods: (i) target-based registration and (ii) surface-based "cloud-to-cloud" registration. The resulting registration accuracies are reported in Tab. 4.

Table 3 Scanning process characteristics for the four scanning plans

	Plan I	Plan II	Plan III	Plan IV
Number of TLS Stations	5	5	5	5
Number of Spherical Targets	8	8	5	7
Number of Flat Targets	13	0	0	0
Field Preparation Time	60 min	25 min	15 min	20 min
Scanning Duration	155 min	155 min	155 min	92 min
Automatic Registration	No	Yes	Yes	Yes

Figure 9 TLS stations labelled ⊗TLS6 and ⊗TLS8

Table 4 Registration accuracy of point clouds using a combined method (target-based registration + "cloud-to-cloud registration")

	Mean Point Error	Maximum Point Error	Minimum Overlap
I Plan (Without optimization)	8.1 mm	10.3 mm	32.9%
II Plan (3D optimization, 3 targets in overlap + tilt compensator)	5.0 mm	7.2 mm	40.0%
III Plan (3D optimization, 2 targets in overlap + tilt compensator)	5.1 mm	8.7 mm	40.0%
IV Plan (3D optimization, 2 targets in overlap + tilt compensator)	5.2 mm	8.8 mm	34.7%

When the two facades of the Faculty of Architecture, Civil Engineering and Geodesy and the Faculty of Forestry were scanned using the non-optimized plan (Plan I) and the optimized plan derived from the proposed methodology

(Plan II), the difference in the mean positional accuracy of points within the registered clouds was 3.1 mm (Tab. 4). In both cases, the scanning duration was identical (155 minutes) and the same number of TLS stations was employed (five). However, the number of scanner targets differed markedly - 21 targets in Plan I versus 8 targets in Plan II - resulting in substantially shorter field setup and data-processing times for the optimized plan.

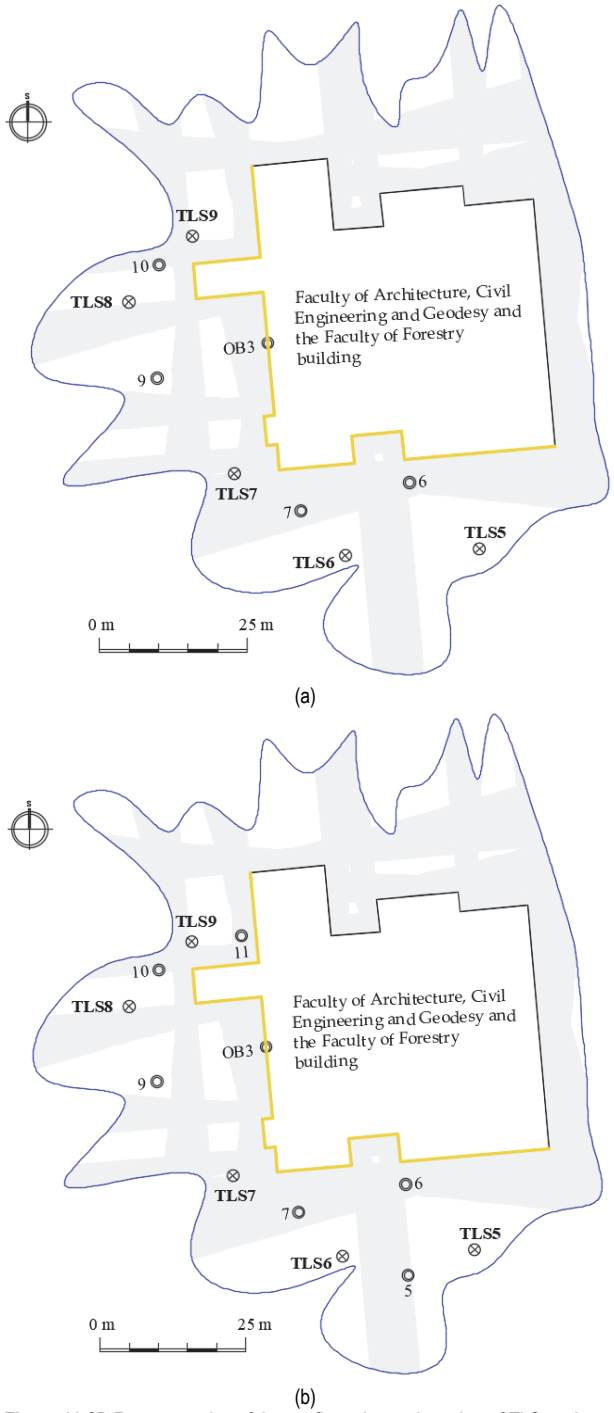

Figure 10 2D Representation of the configuration and number of TLS stations and spherical scanner targets for the (a) third (TLS5, TLS6, TLS7, TLS8, TLS9, 6, 7, 9, 10, OB3) and (b) fourth (TLS5, TLS6, TLS7, TLS8, TLS9, 5, 6, 7, 9, 10, 11, OB3) scanning plans

The registration results for point clouds obtained from the third and fourth scanning plans indicate that, if the terrestrial laser scanner is equipped with a dual-axis tilt compensator, two scanner targets, rather than three, are sufficient within the overlapping zones between adjacent point clouds to ensure reliable registration. For the second, third, and fourth scanning plans, the differences in point cloud registration accuracy parameters were found to be negligible (Tab. 4).

During the processing of data acquired using the second, third, and fourth scanning plans, the software provided an automatic registration option (i.e., the software automatically recognized the scanner targets and performed the registration). This was not the case for Plan I, which required manual intervention, resulting in longer data processing time. Consequently, the availability of automatic registration in the software was included as an additional comparison parameter in Tab. 3.

4 DISCUSSION

As part of this study, the TLS planning process was carried out within a three-dimensional coordinate system, where, in addition to the horizontal positions of TLS stations and scanner targets, the vertical component (height) was also considered.

The planning of terrestrial laser scanning of the building of the Faculty of Architecture, Civil Engineering and Geodesy and the Faculty of Forestry at the University of Banja Luka showed that the selection of TLS station positions is significantly influenced by external obstacles, the complexity of the object's geometry, and instrument constraints related to the minimum and maximum range, as well as the allowable incidence angle of the laser beam. The presence of trees and other objects in the surroundings limited the free zones for scanner placement, which required detailed predefinition of the areas in which scanner placement is permitted.

The conducted analysis of the TLS station layout indicates that, in accordance with predefined technical and geometric criteria, it is possible to achieve full coverage of the scanned object with a minimal number of stations. Specifically, five carefully positioned stations (TLS5-TLS9) enabled coverage of the full length of the two building facades, discretized into 146 segments of 1 m each, achieving a coverage rate of 100%.

The conditions related to the instrument's range, the minimum required overlap between point clouds, and incidence angles were also satisfied. The overlap between adjacent point clouds was considered a key parameter for successful registration and data integration. The value of point cloud overlaps between adjacent stations exceeds 40%, ensuring reliability in the registration process. All distances are within the operational range of the TLS instrument (up to 70 m). The incidence angles, both 2D and 3D, are within the range suitable for satisfactory return signal quality. In the specific case, the maximum allowable incidence angle was adopted as 78°.

In addition, the complexity of the object's facade geometry, which includes protruding and recessed segments, required fragmented determination of the permissible approach zone of TLS stations depending on the maximum allowable value of the incidence angle for each facade segment individually. By intersecting these individual proximity zones, a unified area for TLS placement in relation to the observed side of the object was defined. Despite the more complex geometry of the

building facade and the presence of obstacles such as trees and surrounding structures, a permissible TLS station placement zone was successfully defined.

The analysis of the proposed scanner target layout within the TLS network for scanning two sides of the building's facade showed that the planned eight scanner targets (one on the object and seven in the surroundings) provide stable geometric connectivity and reliable registration of adjacent point clouds. At the overlap between adjacent TLS stations, at least three non-collinear shared scanner targets were positioned, ensuring stable and accurate network connectivity. All quality criteria for assessing the designed network, including internal and external reliability values, marginal detectable error, and the ratios of the semi-axes of the tri-axial error ellipsoid, are within the allowable limits. It is especially important to emphasize that the minimum value of the internal reliability coefficient is 0.30, which is higher than the prescribed minimum, while the mean reliability value is 0.66. The value of the ratio of marginal detectable error to the variance of the observation is 6.22, which is less than the allowed limit, thus satisfying the constraint for gross error detection. The results obtained for the designed configuration of TLS stations and scanner targets show that it is possible to ensure high precision and reliability of point cloud registration through careful design of the network geometry and optimal selection of target types.

In this research, the efficiency and accuracy of four different terrestrial laser scanning (TLS) plans applied to a real object - two facades of the building of the Faculty of Architecture, Civil Engineering and Geodesy and the Faculty of Forestry - were analyzed. The study included all relevant aspects of the process: field preparation, the number and arrangement of TLS stations and scanner targets, total scanning time, the possibility of automatic point cloud registration, as well as qualitative registration parameters (mean and maximum point error, minimum cloud overlap).

The results indicate that applying a scanning optimization methodology based on 3D placement of signal targets and the use of a dual-axis tilt compensator significantly improved the efficiency and accuracy of the process. Compared to the non-optimized plan (First plan), which used 21 scanner targets (8 spherical and 13 flat) and required 60 minutes of field preparation and 155 minutes of scanning, the optimized plans (II, III, and IV) achieved better registration accuracy with significantly fewer resources. Particularly notable is the Fourth plan, in which the total scanning time was reduced by 63 minutes compared to the other plans (to 92 minutes), with minimal reduction in registration precision (Mean Point Error: 5.1 mm; Maximum Point Error: 8.9 mm).

5 CONCLUSIONS

This study demonstrated that proper planning ensures complete scanning of the object, leads to savings in terms of field preparation time, scanning duration, and data processing time, and improves scanning accuracy - an expected outcome given that optimization enables the selection of TLS station locations that satisfy constraints related to scanning geometry (incidence angle and distance).

The planning process, according to the methodology presented in this paper, is largely not automated; at each step, the decision-maker actively participates in the planning process, resulting in a longer time to obtain final results compared to methodologies based on algorithm development. This may hinder the application of the optimization in cases where the scanning subject is the interior of complex structures, such as factories or other industrial facilities with many details. The described optimization methodology primarily applies to planning the scanning of exterior parts of objects and was developed based on the authors' research and experience in the field of terrestrial laser scanning. Future research will focus on further improving the scanning planning methodology and addressing any potential shortcomings not currently evident.

The study could be improved by proposing criteria for selecting a terrestrial laser scanner with optimal measurement characteristics, depending on the specifics of the scanned object (complexity of the structure, maximum allowable proximity to the object depending on the maximum permissible incidence angle of the laser beam, surrounding buildings, trees, and other external obstructions, etc.) and project requirements regarding accuracy.

The results of the study show that careful planning of the TLS station locations and the type and placement of scanner targets (spherical and flat) can ensure high reliability and accuracy in point cloud registration, even under conditions of limited visibility and complex object geometry. A particular contribution of this work lies in the formulation of a methodology that combines facade discretization, identification of geometrically favourable TLS station configurations, and analysis of network reliability and accuracy, thus laying the groundwork for the development of standardized procedures in geospatial documentation of urban structures using TLS technology.

Future research may include the development of automated tools for optimizing the number and layout of TLS stations and scanner targets based on 3D models of terrain and objects, as well as stochastic models for additional quantification of measurement uncertainty, and integration of these procedures within BIM systems.

From an academic and research standpoint, this study aimed to establish the concept of quantitatively managing the trade-off between time, accuracy, and resources in the TLS process. It has been shown that the application of an analytical and modular approach to planning terrestrial laser scanning can significantly enhance the efficiency of field operations and the quality of the collected 3D data.

In conclusion, the proposed optimization of terrestrial laser scanning represents not only a technically feasible and metrologically justified practice but also an economically viable one, with the potential to become a standardized component of modern geodetic and geoinformation methodologies in urban environments.

6 REFERENCES

[1] Azam, A., Alshehri, A., Alharthai, M., El-Banna, M., Yosri, A., & Beshr, A. (2023). Applications of Terrestrial Laser Scanner in Detecting Pavement Surface Defects. *Processes*, *11*(5), 1370-1387. https://doi.org/10.3390/pr11051370

[2] Hu, C., Peng, D., Lv, F., Sun, H., Zhao, T., & Li, W. (2021). Application of Terrestrial Laser Scanner in engineering survey. *IOP Conference Series Earth and Environmental Science*, 783. https://doi.org/10.1088/1755-1315/783/1/012084

[3] Wu, C., Yuan, Y., Tang, Y., & Tian, B. (2021). Application of Terrestrial Laser Scanning (TLS) in the Architecture, Engineering and Construction (AEC) Industry. *Article in Sensors*, *22*(1), 265-296. https://doi.org/10.3390/s22010265

[4] Kekeç, B., Bilim, N., Karakaya, E., & Ghiloufi, D. (2021). Applications of Terrestrial Laser Scanning (Tls) In Mining: a Review. *Turkish Journal of LiDAR*, *3*(1), 31-38. https://doi.org/10.51946/melid.927270

[5] Singh, S. K., Banerjee, B. P., & Raval, S. (2023). A review of laser scanning for geological and geotechnical applications in underground mining. *International Journal of Mining Science and Technology*, *33*(2), 133-154. https://doi.org/10.1016/j.ijmst.2022.09.022

[6] Babić, L., Đapo, A., & Pribićević, B. (2011). Application of a 3D terrestrial laser scanner in industrial applications on the example of objects on gas line "Slobodnica - Donji Miholjac". *5th International Conference on Engineering Surveying*, 71-76.

[7] Fehér, A. (2013). Using 3D Scanners in Archaeology. *Hungarian Archaeology e-Journal.*

[8] Marchand, J., Daniel, S., & Pouliot, J. (2009). Application of Terrestrial Laser Scanning for Knowledge Extraction from Archaeological Excavation. *Geomatica*, *63*(1), 25-36. https://doi.org/10.5623/geomat-2009-0003

[9] Barazzetti, L., Sala, R., Scaioni, M., Cattaneo, C., Gibelli, D., Giussani, A., Poppa, P., Roncoroni, F., & Vandone, A. (2012). 3D scanning and imaging for quick documentation of crime and accident scenes. *Proceedings of SPIE - The International Society for Optical Engineering*, 8359. https://doi.org/10.1117/12.920728

[10] Ares, M., Royo, S., Vidal, J., Campderrós, L., Panyella, D., Pérez, F., Vera, S., & González Ballester, M. (2014). 3D scanning system for in vivo imaging of human body. *Springer*, 899-902. https://doi.org/10.1007/978-3-642-36359-7_168

[11] Cen, Y., Huang, X., Liu, J., Qin, Y., Wu, X., Ye, S., Du, S., & Liao, W. (2024). Application of three-dimensional reconstruction technology in dentistry: a narrative review. *Article in BMC Oral Health*, 23. https://doi.org/10.1186/s12903-023-03142-4

[12] Haleem, A. & Javaid, M. (2019). 3D scanning applications in medical field: A literature-based review. *Clinical Epidemiology and Global Health*, *7*, 199-210. https://doi.org/10.1016/j.cegh.2018.05.006

[13] Javaid, M., Haleem, A., & Kumar, L. (2019). Current status and applications of 3D scanning in dentistry. *Article in Clinical Epidemiology and Global Health*, *7*(2), 228-233. https://doi.org/10.1016/j.cegh.2018.07.005

[14] Rashid, H. (2014). Application of Confocal Laser Scanning Microscopy in Dentistry. *Journal of Advanced Microscopy Research*, *9*(4), 245-252. https://doi.org/10.1166/jamr.2014.1217

[15] Xu, Z., Xu, E., Wu, L., Liu, S., & Mao, Y. (2019). Registration of Terrestrial Laser Scanning Survey Using Terrain-Invariant Regions for Measuring Exploitative Volumes over Open-Pit Mines. *Article in Remote Sensing*, *11*(6), 606-622. https://doi.org/10.3390/rs11060606

[16] Yakar, M., Yilmaz, H. M., & Mutluoglu, O. (2014). Performance of Photogrammetric and Terrestrial Laser Scanning Methods in Volume Computing of Excavtion and Filling Areas. *Arabian Journal for Science and Engineering*, *39*, 387-394. https://doi.org/10.1007/s13369-013-0853-1

[17] Hayakawa, Y. S., Kusumoto, S., & Matta, N. (2016). Application of terrestrial laser scanning for detection of ground surface deformation in small mud volcano (Murono, Japan). *Earth, Planeta and Space*, 68. https://doi.org/10.1186/s40623-016-0495-0

[18] Kasperski, J., Delacourt, C., Allemand, P., Potherat, P., Jaud, M., & Varrel, E. (2010). Application of a Terrestrial Laser Scanner (TLS) to the Study of the Séchilienne Landslide (Isère, France). *Remote Sensing*, *2*(12), 2785-2802. https://doi.org/10.3390/rs122785

[19] Kogut, J. P. & Pilecka, E. (2020). Application of the terrestrial laser scanner in the monitoring of earth structures. *Article in Open Geosciences*, *12* (1), 503-517. https://doi.org/10.1515/geo-2020-0033

[20] Tang, C., Rong, J., Guo, Y., Cai, W., Liang, A., Xu, J., Zhu, W., Tao, X., & Feng, J. (2024). The Application of 3D Laser Scanning Technology in Land Surface Subsidence Monitoring. *Smart Innovation, Systems and Technologies, Publisher: Springer, Singapore*, *388*, 243-252. https://doi.org/10.1007/978-981-97-2144-3_19

[21] Batilović, M., Marković, M., Bulatović, V., Krnić, Đ., & Santrač, N. (2024). Geodetic control of the geometry of the bridge in Kula using terrestrial laser scanning technology. *Proceedings of International Conference on Contemporary Theory and Practice in Construction*, *16*(1), 731-741. https://doi.org/10.61892/stp202401024B

[22] Deruyter, G., Hennau, M., Dewulf, N., & Wolf, V. (2009). Using 3D terrestrial laser scanning as data acquisition technique for the assessment of deviations in geometry between design and as-built models of large structures: a case study. *Proceedings of the 4th international workshop on 3D geo-information*, 101-116.

[23] Marjetič, A. (2018). TPS And TLS Laser Scanning for Measuring the Inclination Of Tall Chimneys. *Journal of the Union of Associations of Geodetic Professionals in Bosnia and Herzegovina - Geodetic Courier*, *49*, 29-43. https://doi.org/10.58817/2233-1786.2018.52.49.29

[24] Soudarissanane, S., Lindenbergh, R., Menenti, M., & Teunissen, P. (2009). Incidence angle influence on the quality of terrestrial laser scanning points. *Proceedings of the ISPRS Workshop Laser scanning*, 183-188.

[25] Pejić, M. (2022). *Terestričko lasersko skeniranje u inženjerstvu*. Građevinski fakultet Univerziteta u Beogradu I Akademska misao, Udžbenik, Beograd.

[26] Aryan, A., Bosche, F., & Tang, P. (2021). Planning for terrestrial laser scanning in construction: A review. *Automation in Construction*, 125. https://doi.org/10.1016/j.autcon.2021.103551

[27] Jia, F. & Lichti, D. (2022). A Practical Algorithm for the Viewpoint Planning of Terrestrial Laser Scanners, *Geomatics*, *2*(2), 181-196. https://doi.org/10.3390/geomatics2020011

[28] Noichl, F., Lichti, D. D., & Borrmann, A. (2024). Automating adaptive scan planning for static laser scanning in complex 3D environments. *Automation in Construction*, 165. https://doi.org/10.1016/j.autcon.2024.105511

[29] Dehbi, Y., Leonhardt, J., Oehrlein, J., & Haunert, J. (2021). Optimal scan planning with enforced network connectivity for the acquisition of three-dimensional indoor models. *ISPRS Journal of Photogrammetry and Remote Sensing*, 180, 103-116. https://doi.org/10.1016/j.isprsjprs.2021.07.013

[30] Jia, F. (2019). *A Model-based, Optimal Design System for Terrestrial Laser Scanning Networks in Complex Sites*. Doctoral thesis, University of Calgary, Department of Geomatics Engineering.

[31] Perović, G., Skorup, D., & Sekulović, D. (2019). *Optimisation of the 2D control geodetic network of the landslide*. In book: *Application of Geographic Information System in Modeling of Natural Catastrophe*. Faculty of Information Technology and Engineering University "Union-Nikola Tesla" in Belgrade, Serbia, 129-159.

[32] Ašanin, S., Pandžić, S., Gospavić, Z., & Milovanović, B. (2007). *Zbirka izabranih zadataka iz inženjerske geodezije*. Beograd.
[33] Jia, F. & Lichti, D. (2019). A Model-Based Design System for Terrestrial Laser Scanning Networks in Complex Sites, *Remote Sensing*, *11*(15). https://doi.org/10.3390/rs11151749
[34] Kaasalainen, S., Jaakkola, A, Kaasalainen, M., Krooks, A., & Kukko, A. (2011). Analysis of Incidence Angle and Distance Effects on Terrestrial Laser Scanner Intensity: Search for Correction Methods. *Remote Sensing*, *3*, 2207-2221. https://doi.org/10.3390/rs3102207
[35] Krooks, A., Kaasalainen, S., Hakala, T., & Nevalainen, O. (2013). Correction of Intensity Incidence Angle Effect in Terrestrial Laser Scanning. *ISPRS Annals of the Photogrammetry, Remote Sensing and Spatial Information Sciences*, *II-5/W2*, 145-150.
[36] Soudarissanane, S., Lindenbergh, R., Menenti, M., & Teunissen, P. (2011). Scanning geometry: Influencing factor on the quality of terrestrial laser scanning points. *ISPRS journal of photogrammetry and remote sensing*, *66*(4), 389-399. https://doi.org/10.1016/j.isprsjprs.2011.01.005
[37] Lichti, D. D. (2007). Error modelling, calibration and analysis of an AM-CW terrestrial laser scanner system. *ISPRS Journal of Photogrammetry and Remote Sensing*, *61*(5), 307-324. https://doi.org/10.1016/j.isprsjprs.2006.10.004
[38] Lichti, D. D., Glennie, C. L., Jahraus, A., & Hartzell, P. (2019). New approach for low-cost TLS target measurement. *Journal of Surveying Engineering*, *145*(3). https://doi.org/10.1061/(ASCE)SU.1943-5428.0000285
[39] Ye, C. & Borenstein, J. (2002). Characterization of a 2-D laser scanner for mobile robot obstacle negotiation. *Proceedings of the IEEE International Conference on Robotics and Automation*.
[40] Mihailović, K. & Aleksić, I. (2008). *Komcepti mreža u geodetskom premeru*. Privredno društvo za kartografiju "GEOKARTA", Beograd.
[41] Soudarissanane, S. & Lindenbergh, R. (2012). Optimizing terrestrial laser scanning measurement set-up. *International Archives of the Photogrammetry, Remote Sensing and Spatial Information Sciences*, *38*, 127-132. https://doi.org/10.5194/isprsarchives-XXXVIII-5-W12-127-2011

Contact information:

Kornelija KLJEČANIN, Teaching Assistant
(Corresponding author)
University of Banja Luka,
Faculty of Architecture, Civil Engineering and Geodesy,
Bulevar vojvode Petra Bojovica 1A, 78000 Banja Luka, Bosnia and Herzegovina
E-mail: kornelija.kljecanin@aggf.unibl.org

Marko PEJIĆ, Associate Professor
University of Belgrade, Faculty of Civil Engineering,
Bulevar kralja Aleksandra 73, 11000 Belgrade, Serbia
E-mail: mpejic@grf.bg.ac.rs